4. Classification of soil and rock

Page 47: Revising of sentence and Table 4.2

The Swedish classification (Rankka et al. 2004) used in Scandinavia is shown in Table 4.2, as well as a similar classification used in parts of Canada. An indication of the sensitivity should be included in the description when a soil is noted to have a large reduction in strength upon remoulding. As there are significant variations in the estimates of sensitivity using the different laboratory and field tests, it is important to identify the testing method used.

Table 4.2. Soil sensitivity

Sensitivity	Ratio of intact to remoulded shear strength, S_t (from Rankka et al. 2004)	Sensitivity	Ratio of intact to remoulded shear strength, S_t (modified from Rosenquist, 1953)
Low	<8	low sensitivity	$S_t < 2$
Medium	8-30	medium sensitivity	$2 < S_t < 4$
High	>30	sensitive	$4 < S_t < 8$
		extra-sensitive, slightly quick	$8 < S_t < 16$
		quick	$S_t > 16$

Page 57: Revision of sentence

Replace:

"Soils containing more than 5% by dry weight of organic matter are considered organic soils and can be classified based on the USCS system as described in Section 4.3.1."

With:

"Soils with sufficient organic matter to influence its properties will be considered an organic soil according to the USCS system described in Section 4.3.1."

5. Site investigations

This chapter discusses site characterization using the self-boring pressuremeter. Use of pressuremeters inserted into pre-bored holes is discussed in the 4th Edition of the CFEM (2006).

9. Deep foundations

Page 249: Revision to sentence following equation 9.6

Replace:

"where q_s is the ultimate shaft resistance (kPa); α is an adhesion factor ranging from ~0.5 to 1.0"

with:

"where q_s is the ultimate shaft resistance (kPa); α is an adhesion factor ranging from ~0.3 to 1.0"

Page 249: Modify equation 9.7 to match Figure 9.1

Replace:

$$\alpha = 0.21 + 0.26\left({}^{p_a}/_{s_u}\right) \qquad (9.7)$$

with:

$$\alpha = 0.21 + 0.26\left({}^{p_a}/_{s_u}\right) \leq 1 \qquad (9.7)$$

Page 252: Modify equation 9.13

Replace:

$$Q_f = \sum \Delta D f_s \Delta L_f \qquad (9.13)$$

with:

$$Q_f = \sum \pi D f_s \Delta L_f \qquad (9.13)$$

Page 254: Modification of Table 9.5 as noted in red

Table 9.5. Bearing capacity factors, kc (after Bustamante and Gianeselli, 1982).

		k_c	
Soil type	q_c (MPa)	Group I	Group II
Soft clay and mud	< 1	0.4	0.5
Moderately compact clay	1 – 5	0.35	0.45
Silt and loose sand	≤ 5	0.4	0.5
Compact to stiff clay and compact silt	> 5	0.45	0.55
Soft chalk	≤ 5	0.2	0.3
Moderately compact sand and gravel	5 – 12	0.4	0.5
Weathered to fragmented chalk	> 5	0.2	0.4
Compact to very compact sand and gravel	> 12	0.3	0.4

Note: Group I: Plain bored piles, mud bored piles, micropiles (grouted under low pressure), cased bored piles, hollow auger-bored piles, piers, and barrettes. Group II: Castin-place screwed piles, driven precast piles, prestressed tubular piles, driven cast piles,
jacked metal piles, micropiles (grouted under high pressure with diameters < 250 mm).

Page 255: Modification of sentence following equation 9.19, as noted in red

where q_s is ultimate unit shaft resistance (kPa); q_t is ultimate unit base resistance (kPa); α is 1 for displacement piles in any soil and non-displacement piles in clays, and 0.5–0.6 for non-displacement piles in granular soils; N_{60} is average SPT value (normalized to 60% energy efficiency) along the pile shaft; N_b is average of SPT values in the vicinity of the pile tip; K_b is ~~is~~ a base factor given in Table 9.7 (Decourt 1995).

Page 285: Modification of Table 9.12, as noted in red.

Table 9.12. Recommended p_m values for simplified analysis (FWHWA-GEC-10), FHWA 2018b).

	Multiplier p_m			
Pile spacing (centre to centre)	3D	4D	5D	6D
Lead row	0.80~~0.70~~	0.90~~0.85~~	1.00~~0.85~~	1.00
Second row	0.40~~0.50~~	0.65	0.85	1.00
Third and higher rows	0.30~~0.35~~	0.50	0.70	1.00

Page 285: Modification of Table 9.13, as noted in red.

Table 9.13. Group effects reduction factors for k_s and n_h ~~(from NAVFAC (1986) DesignManual 7.02)~~ (from CFEM, 1975).

Pile spacing in direction of loading	Subgrade reaction reduction factor, R
8D	1.00
6D	0.70
4D	0.40
3D	0.25

Page 285: Modification of text, as noted in red.

9.10.3.1. General

Ultimate end-bearing resistance is the area of the socket base multiplied by the ultimate bearing pressure. The socket base capacity may be considered to provide the whole socket capacity (Approach 1 described above) or to provide one component of the socket capacity (Approach 3).

Page 286: Modification of text, as noted in red.

~~The method described in Chapter 10 on shallow foundations is applicable to deep foundations.~~ According to Ladanyi and Roy (1971), the effect of depth is included and the formula in terms of allowable or working stress design for bearing pressure on rock becomes

$$q_a = \sigma_c K_{sp} d \tag{9.56}$$

where q_a is allowable bearing pressure (kPa); σ_c is average unconfined compressive strength of the rock core, from ASTM (2007) D2938 (kPa); K_{sp} is an empirical factor~~, as given in Chapter 10 on shallow foundations,~~ which includes a factor of safety of 3; d is a depth factor $=1 + 0.4\left(\frac{L_s}{B_s}\right) \leq 3$, where L_s is depth (length of the socket) (m) and B_s is diameter of the socket (m). K_{sp} can be taken as 0.1 for moderately close rock discontinuity spacing (0.3 to 1 m); 0.25 for wide rock discontinuity spacing (1m to 3m); 0.4 for very wide rock discontinuity spacing (>3m). See CFEM (2006) for additional discussion on K_{sp}.

Page 290: Modification of Figure 9.22: Typo on y-axis.

Fig. 9.22. Load distribution in a rock socket (after Pells and Turner 1979). E_c, elastic modulus for concrete; E_r, elastic modulus for rock.

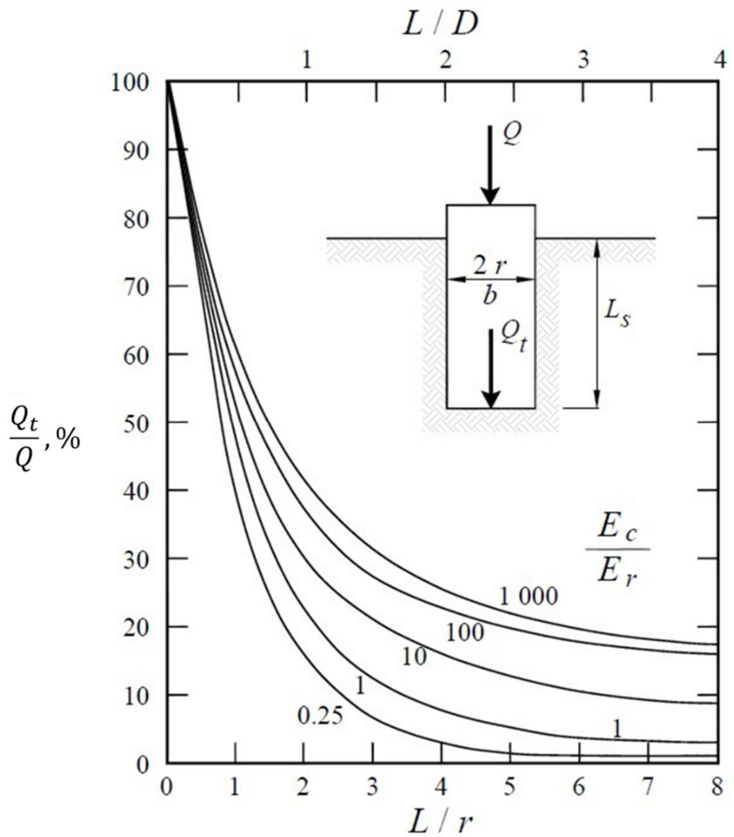

Page 290: Modification of text below equation 9.65, as noted in red.

where q_s is unit socket shear (kPa); $n=Q_t/Q$ is proportion of Q that reaches the socket base, from Fig. 9.22 (dimensionless); Q is total load applied at the top of the socket (kN); L_s is socket length (m); B_s is socket diameter (m).

10. Shallow foundations

Page 348: Modify Equation 10.13, as noted in red.

$$L' = L - 2e_L \tag{10.13}$$

Page 350: Modify text, as noted in red.

Numerical analysis of bearing capacity requires appropriate (i) modelling of boundary conditions, (ii) extent and refinement of finite-element mesh or finite-difference grid, and (iii) selection of constitutive model to capture ground behaviour up to an ultimate limit state. For such nonlinear analyses, the solution needs to progress towards an ultimate limit state with suitably small load or displacement increments. Suitable mesh or grid refinement and load or displacement increments can be readily verified by conducting analyses with progressively increased mesh refinement or decreased increment size until there is negligible change in the numerical solution. Foundation rigidity and interface conditions do not have a significant impact on ultimate bearing capacity for undrained conditions with vertical and concentric loading (Potts et al. 2001), whereas considerations of such soil–structure interactions have a dominant effect on differential settlements and structural resultants of the foundation (e.g., see Section 10.18.2).

Page 351: Add section 10.6.1, as noted in red.

10.6.1 Resistance from bearing on rock

Please consult CFEM (2006) for a discussion related to estimating the bearing pressure of shallow foundations on rock.

14. Frost action

Page 481-482: Modify text below, as noted in red.

The volumetric latent heat term of the soil can be estimated from the following relationship:

$$L_s = \rho_d w L \tag{14.10}$$

where ~~γd~~ ρ_d is the dry ~~unit weight~~ density of the soil (kg/m^3), w is the gravimetric water content of the soil expressed as a fraction and L is the latent heat of fusion of water to ice, which can be taken as ~~334 kJ/kg~~ 334 000 J/kg.

Page 482: Modify text below, as noted in red.

where t is the duration of the freezing period (days) and C is the volumetric heat capacity of the frozen soil C (J/m^{3o}C). C can be calculated as $C = \rho_d(C_s + C_i w)$, where C_s = specific heat of dry soil which can be taken as 710 J/kg^{o}C; C_i = specific heat of ice which can be taken as 2100 J/kg^{o}C; and w = gravimetric water content of the soil (-).

16. Ground improvement and modification

Page 511-512: Modify text, as noted below in red.

Densification of a shallow layer of loose, granular soil can be achieved by application of repeated, dense compaction from the ground surface using conventional compactors such as drum rollers. ~~Depending on the properties of the soil layer at the ground surface and the applied compaction effort, the depth of the improvement can range between 2 and 5 m below the surface from which compaction takes place.~~ The target degree of compaction is highly dependent on the soil type and state of compactness of the soil. The suitability of the soil that immediately underlies the treatment surface for improvement is assessed on the basis of the results of geotechnical exploration and testing.

Page 516: Modify text, as noted below in red.

Deep dynamic compaction (DDC) involves the use of a steel or concrete block tamper typically 10–30 t and dropped in free-fall from heights of up to 30 m using heavy crawler cranes. DDC compacts to depths of as much as 8–10 m, but heavier weights can be utilized to improve soils at greater depths, sometimes to as much as 12–15 m depending on ~~soil~~ ground conditions.

Page 519: Insert text, as noted below in red.

The basic approach of ground improvement using aggregate pier methods is to introduce a tightly packed columnar arrangement of stone (gradation specified by the designer) into the ground to reinforce the soil providing composite ground improvements through the combination of the dense aggregate pier and surrounding improved soil.

18. Earthquake-resistant design

Page 613: Modify text after equation 18.14, as noted in red.

2. Apply fines content correction using eq. 18.14 and Fig. 18.26 to each $(N_1)_{60}$ value

$$(N_1)_{60cs} = (N_1)_{60} + \Delta(N_1)_{60} \tag{18.14}$$

Where $(N_1)_{60cs}$ is the equivalent clean sand normalized SPT value after applying fines content correction; $\Delta(N_1)_{60}$ is the correction in penetration resistance as a function of fines content (FC in percent).

Page 642: Modify equation 18.55 as noted in red.

$$\ldots \quad a3(Ts)^2 + 0.550M_w \pm \epsilon \tag{18.55}$$

19. Unsupported excavations

Page 680: Modify reference, as noted in red.

Leroueil, S. 2001. ~~Cuts and n~~Natural slopes and cuts: movement and failure mechanisms. Géotechnique, 51(3): 195–243. ~~doi:10.1680/geot.2001~~. doi.org/10.1680/geot.2001.51.3.197

20. Soil retaining structures

Page 693: Change Equation 20.8 to that noted in red.

$$Q_{ae} = \frac{1}{2}\gamma H^2(1 - k_v)K_{ae} \tag{20.8}$$

where Q_{ae} is resultant active lateral earth load including static and dynamic loads (kN); γ is unit weight of the soil behind the wall (kN/m^3); H is height of retaining wall (m); k_v is the vertical ~~horizontal~~ earthquake acceleration component as fraction of gravitational acceleration (dimensionless); ….

Page 694: Change Equation 20.9 to that noted in red.

$$K_{ae} = \frac{cos^2(\emptyset' - \theta - i)}{cos(\theta)cos^2(i)cos(\delta + i + \theta)\left[1 + \sqrt{X_a}\right]^2} \tag{20.9}$$

Page 695: Change Equation 20.10 to that noted in red.

$$X_a = \frac{\sin(\emptyset' + \delta)sin(\emptyset' - \theta - \beta)}{cos(\delta + i + \theta)cos(\beta - i)} \tag{20.10}$$

Page 696: Change Equation 20.13 to that noted in red.

$$K_{pe} = \frac{cos^2(\emptyset' - \theta + i)}{cos(\theta)cos^2(i)cos(\delta - i + \theta)\left[1 - \sqrt{X_p}\right]^2} \tag{20.13}$$

Page 696: Change Equation 20.14 to that noted in red.

$$X_p = \frac{\sin(\emptyset' + \delta) sin(\emptyset' - \theta + \beta)}{cos(\delta - i + \theta) cos(\beta - i)} \tag{20.14}$$

Page 696: Modify paragraph, as noted in red below.

The Mononabe–Okabe determination of the active and passive earth pressures does not provide any indication of the distribution of the loads. The reader should consult Chapter 18 for a discussion of the distribution of this load. ~~It is considered that the increases in active and passive incremental earthquake pressures are greater near the top of the wall. Therefore, it is common to apply the resultant incremental earthquake loads at a height of 0.6H, where H is the height above the bottom of the wall.~~

Page 704: Modify Figure caption for Figure 20.14, as noted in red below.

Figure 20.14 (a) should read $K_o\sigma'_{z=H}$ in the subscript of the AT REST figure, where $K_o\sigma'_{z=H}$ is the horizontal effective stress behind the wall at depth z=H.

22. Groundwater control

Page 712: Modify paragraph, as noted in red below.

As the potential for bottom instability increases, the heave in the base of the excavation and movement surrounding the excavation increase and FS_b decreases. In the case of soft clays underlying the base of an excavation where FS_b is smaller than 2, substantial deformations of the excavation support, base and surrounding ground may occur. Where FS_b is less than 1.5, the depth of penetration of the support system should extend below the base of the excavation. The force on the buried section of wall can be calculated according to Fig. 20.21 and Section 20.2. ~~Section 20.3.~~

Page 757: Add text to discussion, as noted in red.

A minimum FS value of 1.1 has been reported by Frank et al. (2005) for this failure mode. They also provide guidance on the use of load and resistance factors for this failure mode. In the previous versions of the CFEM, the safety margin was achieved by limiting the pore pressure to 70% of the total stress, which would equate to a FS of 1.43. The global factor of safety in eq. 22.5 should be based on the judgment and experience of a groundwater specialist. It should depend on the consequences of failure and the uncertainty in determining σ_v and u. The global FS may be reduced for narrow excavations if the shear strength of the clay or the friction along the seepage cut-off can be relied upon as a significant contributor to uplift resistance. Lower values of FS may also be adopted if the pore pressure in the underlying aquifer is carefully monitored and controlled during construction. An example of this approach is described in the detailed case study of McRostie et al. (1996).

Approaches described in this section are based on the simplification of Figure 22.2 and may not cover all situations encountered in practice, as soil and groundwater conditions may be complex and involve multiple soil layers and/or preferential drainage paths (e.g. sand/silt partings or fractured soil). In these cases, good understanding of the ground conditions is required before being used as input to more sophisticated numerical analyses (e.g. Burland and Hancock, 1977).

Page 759: Modify Equation 22.13, as noted in red.

$$\varphi_1 \cong 0.43exp\left[\left(\frac{5}{3}\right)\left(\frac{d_2}{T_2}\right)\right] \tag{22.13}$$

23. Drainage and filter design

Page 781: Modify paragraphs, as noted in red below.

Where the drainage level is below that of the prevailing groundwater, it will permanently lower the groundwater in the vicinity of the drain. The shape of the drawdown in the phreatic surface around a building will be irregular, but will generally be perpendicular to the wall. It can be visualized as a section through a cone. The distance from the building wall at which the drain has no significant drawdown effect is described as the radius of influence and the area within this dimension is the zone of influence. It should be noted that for complicated ground conditions, numerical modelling can be performed to assess this zone of influence with proper inputs of boundary conditions, soil properties and problem geometry.

Approximations for the zone of influence for routine cases can be made with simple empirical approaches. Unlike calculations for wells where the duration of pumping and flow can vary, a drainage system is a steady-state long-term situation. The rate at which water enters the system is the flow under gravity. The primary parameters that govern the zone of influence are therefore the change in head (the depth of the drainage level below the prevailing groundwater level) and the hydraulic conductivity of the soil. An empirical relationship to estimate the radius of influence was developed by Kyieleis and Sichardt (1930) as shown in eq. 23.1.

Added References

Burland, J.B. and Hancock, R.J.R., 1977. Geotechnical aspects of the design for the underground car park at the Palace of Westminster, London. *Structural Engineer*, *55*(2), pp.87-100.